Development 126, 5027-5040 (1999)
Printed in Great Britain © The Company of Biologists Limited 1999
DEV2452

Mice mutant for both *Hoxa1* and *Hoxb1* show extensive remodeling of the hindbrain and defects in craniofacial development

Mireille Rossel* and Mario R. Capecchi‡

Howard Hughes Medical Institute, Department of Human Genetics, University of Utah School of Medicine, Salt Lake City, Utah 84112, USA

*Present address: Laboratoire de Génétique, Domaine Rockefeller, Université Claude Bernard Lyon 1, Lyon Cedex 08, France

‡Author for correspondence (e-mail: mario.capecchi@genetics.utah.edu)

Accepted 7 September; published on WWW 21 October 1999

SUMMARY

The analysis of mice mutant for both *Hoxa1* and *Hoxb1* suggests that these two genes function together to pattern the hindbrain. Separately, mutations in *Hoxa1* and *Hoxb1* have profoundly different effects on hindbrain development. *Hoxa1* mutations disrupt the rhombomeric organization of the hindbrain, whereas *Hoxb1* mutations do not alter the rhombomeric pattern, but instead influence the fate of cells originating in rhombomere 4. We suggest that these differences are not the consequences of different functional roles for these gene products, but rather reflect differences in the kinetics of *Hoxa1* and *Hoxb1* gene expression. In strong support of the idea that *Hoxa1* and *Hoxb1* have overlapping functions, *Hoxa1/Hoxb1* double mutant homozygotes exhibit a plethora of defects either not seen, or seen only in a very mild form, in mice mutant for only *Hoxa1* or *Hoxb1*. Examples include: the loss of both rhombomeres 4 and 5, the selective loss of the 2nd branchial arch, and the loss of most, but not all, 2nd branchial arch-derived tissues. We suggest that the early role for both of these genes in hindbrain development is specification of rhombomere identities and that the aberrant development of the hindbrain in *Hoxa1/Hoxb1* double mutants proceeds through two phases, the misspecification of rhombomeres within the hindbrain, followed subsequently by size regulation of the misspecified hindbrain through induction of apoptosis.

Key words: *Hoxa1*, *Hoxb1*, Hindbrain, Craniofacial development, Branchial arch, Rhombomere

INTRODUCTION

Early in its development, the vertebrate hindbrain is transiently subdivided along its rostrocaudal axis into seven or eight metameric segments called rhombomeres (Lumsden and Keynes, 1989). Rhombomeres can function as compartments that limit cell movement and thereby create centers that are capable of independent development and diversification through localized gene activity and cell interactions (Fraser et al., 1990). Segmentation and diversification of the rhombomeres confers periodicity on the hindbrain. For example, the even numbered rhombomeres (r2, 4 and 6) contain the exit points for the Vth, VIIth and IXth cranial nerves that innervate the 1st, 2nd and 3rd branchial arches, respectively (Lumsden and Keynes, 1989). The segmental organization of the hindbrain also profoundly influences craniofacial development by providing the source of patterned neural crest cells that populate the branchial arches. The majority of neural crest cells that migrate into the 1st, 2nd and 3rd branchial arches emanate as discrete populations of cells from the 2nd, 4th and 6th rhombomeres, respectively (Lumsden et al., 1991). Following their migration into the branchial arches, neural crest cells then proceed to pattern the branchial arch-derived tissues (Le Lievre and Le Douarin, 1975; Noden, 1983a,b; Gendron-Maguire et al., 1993; Rijli et al., 1993; Köntges and Lumsden, 1996; Manley and Capecchi, 1997, 1998; Gavalas et al., 1998; Studer et al., 1998).

Rhombomeres and the neural crest that emanate from these rhombomeres can be distinguished by their patterns of gene expression. These gene products (RNA and protein) can in turn be used as molecular markers to distinguish rhombomere and neural crest identities. Among genes that are expressed in specific rhombomeres are transcription factors, such as the *Hox* genes, *Krox-20* and *kreisler*, as well as tyrosine kinase receptors such as members of the Eph family. Each rhombomere and neural crest cell population is characterized by a unique combination of *Hox* gene expression (Hunt et al., 1991, Hunt and Krumlauf, 1991). Mutational analysis has demonstrated that the transcription factors *Hoxa1* (Carpenter et al., 1993; Mark et al., 1993), *Krox-20* (Schneider-Maunoury et al., 1993; Helmbacher et al., 1998) and *kreisler* (Cordes and Barsh, 1994; McKay et al., 1994) are required for the specification and/or maintenance of specific rhombomeres.

It is interesting that the phenotypic consequences of separately disrupting the two paralogous *Hox* genes, *Hoxa1* and *Hoxb1*, are so different. *Hoxa1* mutant homozygous mice

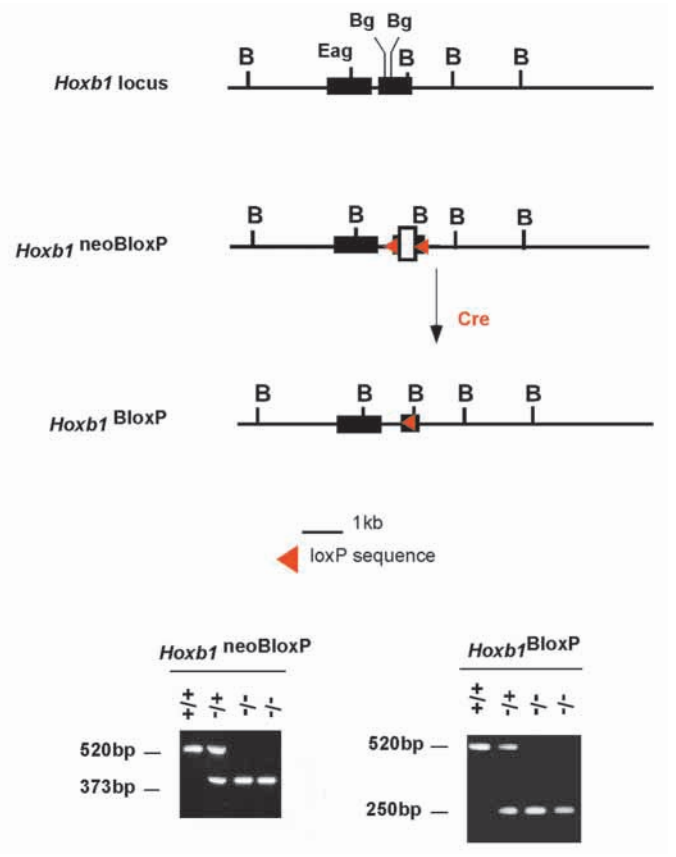

Fig. 1. The *Hoxb1*^{Blox} allele. (Top line) The wild-type *Hoxb1* locus. (Middle line) The *Hoxb1*^{neoBloxP} locus. Note that the *Hoxb1* gene has a *Bam*HI linker mutation inserted at the *Eag*I site in the 1st exon of *Hoxb1* and a loxP neo loxP cassette that replaces a 317 bp *Bgl*II fragment within exon 2. The structure of this targeted allele was assessed by Southern transfer analysis as described for the *Hoxb1*^{neoB} allele in Goddard et al., 1996. (Lower line) Following CRE-mediated site-specific recombination between the *loxP* sites flanking the *neo* gene, a single *loxP* site is retained within the second exon of *Hoxb1*. The removal of the *neo* gene was assessed by Southern transfer analysis, as well as by the PCR based assay shown above.

show major perturbation in hindbrain organization. For example, the 5th rhombomere appears to be entirely (Carpenter et al., 1993) or largely (Mark et al., 1993) missing in *Hoxa1* mutant homozygotes. The 4th rhombomere is also defective, being smaller than normal, and the neural crest population derived from the 4th rhombomere appears to be compromised since neural crest structures derived from the 2nd branchial arch are hypoplastic (Lufkin et al., 1991; Chisaka et al., 1992; Carpenter et al., 1993; Mark et al., 1993). On the contrary, *Hoxb1* mutant embryos show no overt defects in the organization of rhombomeres, nor do they exhibit any defects in neural crest-derived tissues. Rather, targeted disruption of *Hoxb1* appears to affect only the identity of neurons specified in the fourth rhombomere (Goddard et al., 1996; Studer et al., 1996). The remarkable differences in the mutant phenotypes seen in *Hoxa1* and *Hoxb1* mutant mice suggest separate roles for these two genes during hindbrain development. However, we will argue that the very different phenotypic outcomes resulting from these two mutations can be understood in terms of similar functions. In support of this hypothesis, in mice mutant for both *Hox* genes, the mutations show extensive exacerbation of each other's abnormal phenotypes. Thus, *Hoxa1/Hoxb1* double mutant embryos exhibit not only loss of rhombomere 5, but also of rhombomere 4. Furthermore, neural crest-derived tissues of the 2nd branchial arch are not simply reduced in size, but are missing, as is the entire 2nd branchial arch. The dramatic extensions of the defects seen in the organization of the hindbrain and in the formation of the 2nd branchial arch neural crest-derived tissues argue for commonality of purpose, and/or for extensive overlap of function between these two paralogous *Hox* genes.

During the course of this work, two studies have reported on the effect of co-disrupting *Hoxa1* and *Hoxb1* on hindbrain development (Gavalas et al., 1998; Studer et al., 1998). They described the inability to specify and/or maintain a major portion of the 4th rhombomere in the double mutants. They established that *Hoxb1* expression in r4 is partially under the control of *Hoxa1*, and that *Hoxa1* and *Hoxb1* expression is induced by endogenous retinoids. The hindbrain and branchial arch defects that we observe in *Hoxa1/Hoxb1* double mutant embryos are in good agreement with those reported by Gavalas et al. (1998) and Studer et al. (1998), except that our double mutant phenotype is more severe. We observe a complete loss of the 4th and 5th rhombomeres, rather than the almost complete loss of both rhombomeres. This difference probably reflects differences in the nature of the loss-of-function mutations introduced into these *Hox* genes. We report that formation of the 2nd and 3rd branchial pouches and their derived tissues are also affected in *Hoxa1/Hoxb1* double mutants, as is the formation of lungs. We extended the analysis of the *Hoxa1/Hoxb1* double mutant to include a description on the effect of these mutations on the formation of the facial muscles.

We suggest that the loss of rhombomere organization observed in *Hoxa1* mutants, and extended in *Hoxa1/Hoxb1* double mutants, is a consequence of a combination of initial misspecification of rhombomeres, followed by remodeling of the misspecified hindbrain by apoptosis. In this view, the initial roles for both *Hoxa1* and *Hoxb1* during hindbrain development are similar. They both function to specify rhombomere identity. One reason for the more extensive consequences on hindbrain development of individually disrupting *Hoxa1* compared to *Hoxb1*, is that *Hoxa1* is also required to set the anterior boundary of *Hoxb1* expression (J. R. Barrow, H. S. Stadler, J. M. Goddard and M. C., unpublished results). As a consequence, mutations in *Hoxa1* not only eliminate *Hoxa1* function, but also influence the region of the hindbrain where *Hoxb1* is active. Within the region that no longer expresses *Hoxb1*, neither paralogous gene is functional, placing this region in double jeopardy.

The lack of formation of the 2nd branchial arch and derivative pouches seen in *Hoxa1/Hoxb1* double mutants may follow from the absence of an r4 domain, the source of r4-derived neural crest. The absence of r4-derived neural crest may in turn result in the failure to produce the 2nd branchial arch, the 2nd branchial arch-derived tissues, as well as 2nd and 3rd branchial pouch-derived tissues. This double mutant phenotype provides a clear example in which a failure in segmental organization of the hindbrain initiates a cascade of tissue misalignments that profoundly affect subsequent craniofacial development.

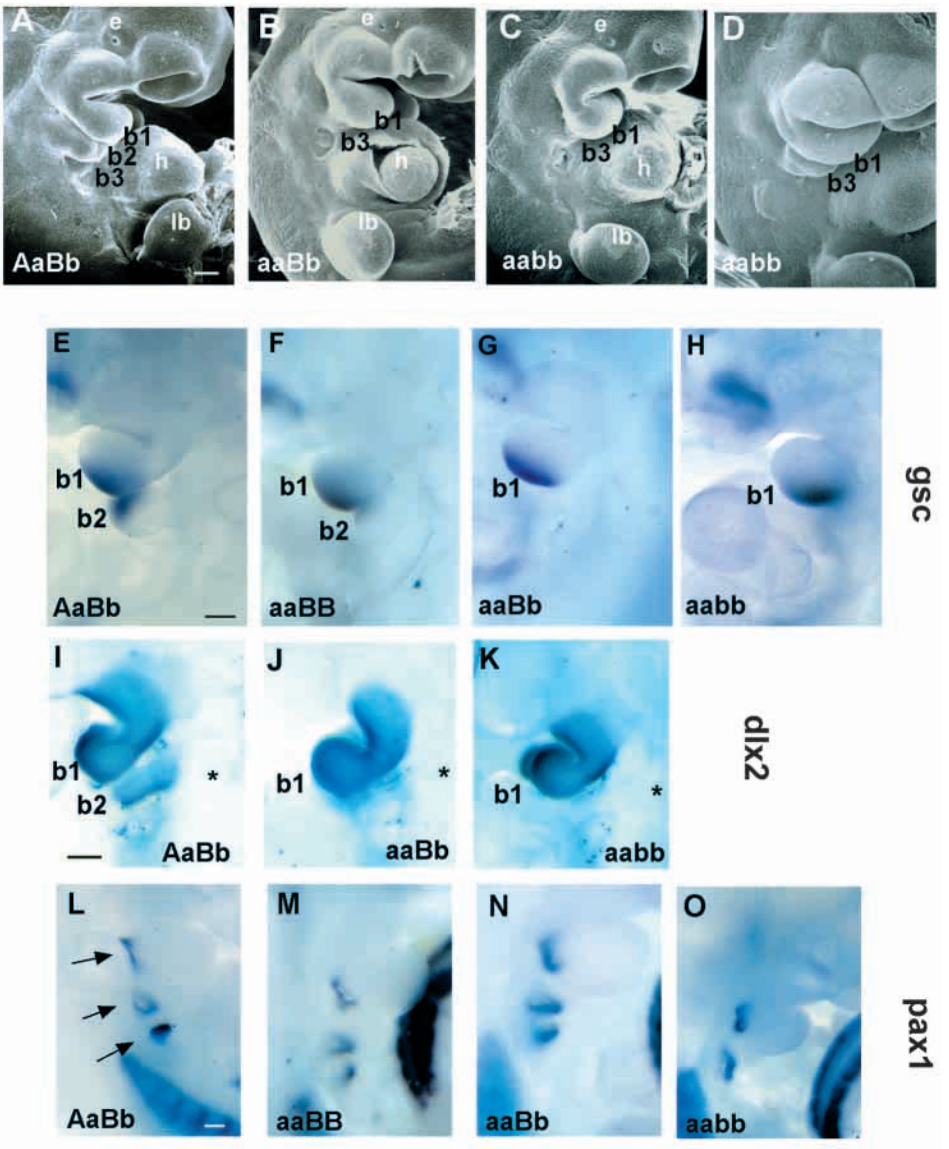

Fig. 2. Lack of the 2nd branchial arch in *Hoxa1/Hoxb1* double mutants and defects in the formation of the 2nd and 3rd branchial pouches. (A-D) Scanning electron microscopic views of the branchial arches of E10.5 (A-C) and E11 (D) mouse embryos. The genotype of the embryo is denoted in the lower left-hand corner where A,B denotes the wild-type and a,b the mutant alleles of *Hoxa1* and *Hoxb1*, respectively. At E10.5 the branchial arches, b1, b2 and b3, are evident in control embryos (A). However, in aaBb or aabb embryos, only two branchial arches, b1 and b3, are evident. The absence of the 2nd branchial arch in aabb embryos is also evident at later stages (D). (E-H) Embryos labeled by whole-mount, in situ hybridization using an RNA probe for *goosecoid* (*gsc*). The *gsc* probe labels the 1st and 2nd branchial arches evident in control (AaBb) and *Hoxa1* (aaBB) mutant embryos. No labeling of the 2nd branchial arch is evident in aaBb (G) or aabb (H) embryos. (I) *Distaless* x2 (*dlx2*) is expressed in post-migratory neural crest cells in the 1st and 2nd branchial arches. (J) In aaBb and (K) aabb embryos, strong labeling is observed in the 1st branchial arch, but no labeling is seen in the region normally occupied by the 2nd branchial arch. (L) *Pax1* is normally expressed in the endoderm of the branchial pouches 1-3. (M) The pattern of *pax1* expression in aaBB embryos is indistinguishable compared to control embryos. (N) In aaBb embryos the position of the 2nd and 3rd branchial pouches is shifted towards the 1st branchial pouch. (O) In aabb embryos the 2nd branchial pouch is missing and the shape of the 3rd pouch is distorted relative to controls. e, eye; h, heart; lb, limb bud; b1, b2 and b3, 1st, 2nd and 3rd branchial arches. The asterisk in I-K marks the position of the otocyst. Scale bar, 200 μm.

MATERIALS AND METHODS

Mutant alleles of *Hoxb1* and *Hoxa1*

The *Hoxb1* loss-of-function alleles that have been described (Goddard et al., 1996; Studer et al., 1996) differ significantly from each other. For example, whereas the majority of *Hoxb1* mutant homozygotes reported by Goddard et al. (1996) are viable, mice with the Studer mutant allele die at birth. Goddard et al. (1996) reported on two mutant alleles, $Hoxb1^{neo}$ and $Hoxb1^{Bneo}$, both of which contain neo^r insertions (pMC1neo) in the second exon. In addition, the $Hoxb1^{Bneo}$ allele contains a *Bam*HI linker mutation in the first exon that disrupts those coding sequences as well. Mice homozygous for these two mutant alleles do not differ significantly. The only distinguishable feature of the mutant phenotype is that 98% of the $Hoxb1^{neo}$ mutant homozygotes survive at birth versus a 94% survival of $Hoxb1^{Bneo}$ homozygotes. The Studer allele contains a β-galactosidase-neo^r (pGKneo) insertion in the first exon of *Hoxb1*.

In order to determine whether the presence of the neo^r gene in the $Hoxb1^{Bneo}$ allele influences the mutant phenotype, the neo^r gene was flanked with *loxP* sites and the neo^r sequences were removed by CRE-mediated site-specific recombination (Araki et al., 1995; see Fig. 1). We designate this allele as $Hoxb1^{BloxP}$. Following CRE-mediated recombination, one *loxP* site remains in the second exon of *Hoxb1*. This allele therefore contains out-of-frame disruptions in both the first and second exons (i.e., *Bam*HI and *loxP* site, respectively). The mutant phenotype of $Hoxb1^{BloxP}$ homozygotes is indistinguishable from $Hoxb1^{Bneo}$ homozygotes, demonstrating that *pMC1neo* cassette in the second exon of each of the Goddard *Hoxb1* alleles had no apparent effects on the function of adjacent *Hox* genes. The studies described in this paper used mice containing the $Hoxb1^{BloxP}$ allele.

We have also generated an allele of *Hoxa1* in which the *neo^r* gene inserted for selection was subsequently removed from the *Hoxa1* locus (Godwin et al., 1998). In this mutant *Hoxa1* allele, the gene encoding the green fluorescent protein (GFP) was fused, in frame with *Hoxa1*, at the unique *Aat*II site in exon 1. The *neo^r* gene was flanked with *loxP* sites, which allowed its subsequent removal from the mouse germline by mating with mice expressing the CRE recombinase (Schwenk et al., 1995). The mutant phenotype associated with homozygosity for this allele, $Hoxa1^{GFPloxP}$, was found to be indistinguishable from the phenotype previously reported for our $Hoxa1^{neo}$ allele (Chisaka et al., 1992; Carpenter et al., 1993; H. S. Stadler and M. C., unpublished results). This demonstrates that the pMC1neo insertion into the 2nd exon of *Hoxa1* does not influence the function of surrounding genes. Most of the studies reported in this

paper, however, used the original *Hoxa1*^{neo} allele described by Chisaka et al. (1992).

The mutant phenotypes resulting from loss-of-function alleles of *Hoxa1* produced by Lufkin et al. (1991) and Chisaka et al. (1992) also differ. For example, with the Chisaka allele, Carpenter et al. (1993) describe a complete absence of expression of r5 molecular markers in *Hoxa1* mutant homozygous embryos, whereas Mark et al. (1993), using the Lufkin allele, observed a remnant of r5-*Krox20* expression, suggesting that a trace of rhombomere 5 is retained in their mutant homozygotes. This difference was attributed to the differences in the sites of insertion of the *neo*^{r} gene. In the Chisaka et al. (1992) allele, pMC1 neo disrupts the *Hoxa1* homeodomain in the 2nd exon. Lufkin et al. (1991), however, inserted a neo^r cassette into the first exon of *Hoxa1*. Two transcripts are produced from the *Hoxa1* locus (La Rosa and Gudas, 1988) by alternative splicing. One transcript encodes the entire protein. The second transcript encodes only the NH_2-terminal portion of the protein (i.e., it lacks the homeodomain). The Chisaka allele disrupts only the first transcript, whereas the Lufkin allele disrupts both transcripts. It has been hypothesized that the transcript that encodes the NH_2-terminal fragment of *Hoxa1* may produce a product that interferes with normal *Hoxa1,* and possibly even *Hoxb1,* functions. In that case, the Chisaka allele could represent a more severe loss-of-function allele than the Lufkin allele, because the former does not affect the production of the shorter repressive transcript. The insertion point of the *Hoxa1*^{GFPlox} allele does disrupt the 3′ end of the shorter transcript and, as already stated, the mutant phenotype associated with this allele cannot be distinguished from the Chisaka allele. This argues that if the shorter transcript has a biological function, then the 3′ end of the shorter transcript cannot contribute to the mutant phenotype. Further, since removal of the *neo*^{r} gene from this allele does not alter the *Hoxa1* mutant phenotype, it cannot be contributing to the mutant phenotype either.

Histology

Animals were processed for paraffin sections as previously described (Goddard et al., 1996.) 10 μm sections from mutant and control newborns were stained with Hematoxylin and Eosin, mounted in DPX and photographed as previously described (Mansour et al., 1993).

Immunohistochemistry

Whole-mount detection of neurofilament protein was performed with the 2H3 antibody directed against the 155 kDa subunit of the neurofilament protein (Dodd et al., 1988) as previously described (Chisaka and Capecchi, 1991). Immunostaining of Hoxb1 and Krox-20 proteins was performed with secondary anti-rabbit antibody conjugated, respectively, to Texas red (Molecular probes, Eugene Oregon) or to FITC (Jackson Labs), and carried out either with separate samples (Goddard et al., 1996) or sequentially with samples for double labeling (Barrow et al., 1999).

Immunolocalization of the CRABP1 protein was performed as previously described (Manley and Capecchi, 1995) with a polyclonal antibody generously provided by U. Eriksson (Eriksson et al., 1987) that was detected with an FITC-conjugated, anti-rabbit secondary antibody (Jackson Laboratories).

RNA in situ hybridization

Whole-mount, in situ hybridization was performed as described (Carpenter et al., 1993; Manley and Capecchi, 1995). For in situ hybridization followed by immunostaining, no proteinase K treatment was applied. The embryos were refixed with 4% paraformaldehyde prior to incubation with the primary antibody directed against Krox-20.

The following probes were used for whole-mount, in situ hybridization. The *Hoxa3* probe was a 650 bp *Eco*RI cDNA fragment containing the first coding exon and the homeobox; the *Pax1* probe was a 1 kb cDNA fragment previously described (Manley and Capecchi, 1995), generously provided by R. Balling. The *Hmx1* probe was a 280 bp *Sma*I-*Bam*HI fragment from the 3′ UTR, generously provided by K. Yoshiura. The *EphA4* probe was a 1200 bp *Eco*RI-*Bam*HI fragment generously provided by F. Helmbacher. The *AP-2* probe was a 500 bp *Bam*HI-*Hin*dIII cDNA fragment, corresponding to the C-terminal region of the protein, generously provided by P. Mitchell. The *distaless x2 (dlx2)* probe was a 2.4 kb cDNA fragment generously provided by J. L. Rubinstein (Porteus et al., 1992). The *Gsc* probe was a *Pst*I-*Hin*cII fragment of 909 bp (Blum et al., 1992). The *Krox-20* probe was a 990 bp, *Apa*I-*Sca*I fragment (Carpenter et al., 1993). *Kreisler* probe was a 490 bp *Hin*dIII-*Eco*RI fragment kindly provided by S. Cordes. The *Hoxb2* probe was a 900 bp *Pst*I-*Hin*dIII fragment isolated from a cDNA clone, containing 130 bp of 3′ coding sequence and extending into the 3′ UTR.

Scanning electron microscopy

Embryos were fixed in the dark in a 1% aqueous osmium tetroxide solution (Polysciences, Inc.) for 4 hours, rinsed, dehydrated through an ethanol series (20,50,80,100%), critical point dried and sputter-coated with 60/40 gold/palladium alloy. Specimens were placed on mounts by use of double-stick tape and examined in a Hitachi S-450 scanning electron microscope at a working distance of 15 mm at 15 kV and a magnification of ×50. Images were recorded on Polaroid 55P/N film.

Cell death determination

Apoptotic cells were detected using terminal transferase dUTP-biotin nick-end labeling (TUNEL) on whole-mount embryos as described by Maden et al. (1997). Texas-Red-conjugated streptavidin was used to measure biotin incorporation (Boehringer Mannheim). The fluorescent signal was visualized by confocal microscopy. For each age group, four embryos of each genotype were examined by TUNEL assays to determine the extent of apoptosis in these embryos.

Cell proliferation analysis

The relative number of cells in S-phase was determined by immunohistochemical detection of 5′ bromodeoxyuridine (BrdU) incorporation (Boehringer Mannheim). Briefly, pregnant mice were injected intraperitoneally with a solution of 10 mg/ml BrdU in PBS at a final concentration of 1 mg BrdU per gram of mouse body weight. After 1 hour, the embryos were collected, fixed in 4% paraformaldehyde overnight at 4°C, rinsed, embedded in paraffin and sectioned (5 μm). The sections were reacted with BrdU antisera according to manufacturer recommendations (Boehringer Mannheim). Two embryos of each genotype and at each time point were sectioned and processed for BrdU analysis.

RESULTS

Genotypes

In order to simplify discussion of genotypes, we will use A, B and a, b to designate the wild-type and mutant alleles (see Materials and Methods) of *Hoxa1* and *Hoxb1*, respectively. Thus, for example, aabb designates the genotype of *Hoxa1/Hoxb1* double mutant homozygotes (*Hoxa1*$^{-/-}$*; Hoxb1*$^{-/-}$).

AAbb, AaBb and Aabb mice are viable and fertile, whereas aaBB, aaBb and aabb mice die at birth. Aabb mice show VIIth nerve defects indistinguishable from those seen in AAbb mice (Goddard et al., 1996). Thus, removal of one functional copy of *Hoxa1* from *Hoxb1* mutant homozygotes does not appear to measurably exacerbate the VIIth nerve defects seen in AAbb mice. Further, with respect to morphology and molecular markers expressed within the hindbrain, branchial arches and branchial pouches, no differences between embryos with the

AAbb, AaBb and Aabb genotypes were discernible. However, removal of one functional allele of *Hoxb1* from *Hoxa1* mutant homozygotes greatly exacerbates the *Hoxa1* mutant defects and generates new defects not seen in aaBB mice. Thus, for the purpose of this paper, the principal genotypes that will be compared include: controls (wild type [AABB] or mice heterozygous for mutations in both genes [AaBb]), with aaBb and aabb mice.

Second branchial arch defects

Although *Hoxb1* is prominently expressed in neural crest emanating from the 4th rhombomere and migrating into the second branchial arch, *Hoxb1* mutant homozygotes show no defects in 2nd branchial arch neural crest-derived structures (Goddard et al., 1996; Studer et al., 1996). *Hoxa1* mutants, on the contrary, exhibit hypoplasia of 2nd branchial arch-derived tissues (Lufkin et al., 1991; Chisaka et al., 1992; Barrow and Capecchi, 1999). However, the expressivity of this mutant phenotype is highly variable, suggesting that other *Hox* genes may be overlapping with *Hoxa1* in regulating this neural crest population. Hypoplasia of the 2nd branchial arch is barely perceptible in *Hoxa1* mutant homozygotes. However, removal of one copy of the *Hoxb1* gene from *Hoxa1* mutant homozygotes (i.e., aaBb mice) results in the elimination of the 2nd branchial arch. This can be seen morphologically using scanning electron microscopy (SEM), and by the use of molecular markers expressed within the branchial arches (Fig. 2). No overt signs of a 2nd branchial arch were visible by SEM in either aaBb or aabb embryos from E9.0 to E11.5 (Fig. 2B-D). In the absence of a 2nd branchial arch, the 3rd branchial arch is now at the position of the 2nd arch. As judged by SEM, the development of the 3rd and 4th branchial arches appears normal at E11.5 in aaBb and aabb embryos. The absence of the 2nd branchial arch in aaBb and aabb embryos has also been confirmed by extensive histological analysis (data not shown).

Goosecoid (*gsc*) is expressed in the posterior portion of the 1st branchial arch and in the anterior portion of the second arch in control embryos (Gaunt et al., 1993; Fig. 2E). Consistent with the absence of 2nd branchial arch in aaBb and aabb embryos, *gsc* expression is not discernible at the normal position of the 2nd branchial arch (Fig. 2G,H). *Dlx2* is also strongly expressed in the 1st and 2nd branchial arches (Zhang et al., 1996; Fig. 2I). No 2nd branchial arch, *dlx2* expression is seen in aaBb and aabb embryos (Fig. 2J,K). We have also examined a series of other molecular markers normally expressed in the branchial arches, such as *hmx-1*, *FGF3* and *Hoxa3* (data not shown). The conclusion derived from all of these experiments is that the 2nd branchial arch is selectively missing in aaBb and aabb mutant embryos. These experiments demonstrate that, although *Hoxb1* mutant homozygotes (AAbb) show no defects in the formation of the 2nd branchial arch, or in any neural crest-derived tissues, *Hoxb1* does have a prominent role in the formation of these tissues that is only observed in the absence of *Hoxa1* function. In *Hoxa1* mutant homozygotes, where a deficiency in 2nd branchial arch formation is barely detectable, removal of a single functional copy of *Hoxb1* results in complete absence of this arch. The simplest hypothesis is that in the absence of both functional copies of *Hoxa1* and one functional copy of *Hoxb1*, there is insufficient r4-derived neural crest to sustain formation of the 2nd branchial arch. The effect of the *Hoxa1* mutation on this neural crest population must be inflicted prior to neural crest migration, since *Hoxa1* ceases to be expressed in the head region before migration of this neural crest population begins. With respect to *Hoxb1* expression, ectodermal and mesodermal expression in the head region also ceases by E8.5; however, a strong stripe of *Hoxb1* expression is activated and maintained in the cells of the neural tube at the level of rhombomere 4, and in the neural crest emanating from this region (Frohman et al., 1990; Murphy and Hill, 1991; Hunt et al., 1991, Hunt and Krumlauf, 1991).

Branchial pouch defects

Since the 2nd branchial arch is not formed in aaBb and aabb mice, we wished to determine if these mutations also affect the formation of the branchial pouches. *Pax1* is expressed in the endoderm of the 1st, 2nd and 3rd branchial pouches at E10.5 (Wallin et al., 1996; Fig. 2L,M). Except for a slight shift in the position of the 2nd and 3rd branchial pouches towards the 1st branchial pouch, formation of these pouches appears fairly normal in aaBb embryos (Fig. 2N). However, this phenotype is variable. Even in the same aaBb embryo, the shapes of the 2nd and 3rd branchial pouches can be normal on one side and distorted on the opposing side. In aabb embryos, the 2nd pouch is always missing (Fig. 2O) and the shape of the 3rd arch is distorted. Histological analysis shows that the endoderm of the 1st and 3rd branchial pouches is contiguous in aabb embryos, indicating that the 2nd pouch endoderm is missing in these mutants as opposed to being involuted or fused with the adjacent pouch endoderm (data not shown). Further confirmation that formation of the branchial pouches is abnormal in aabb embryos was obtained by examination of the *FGF3* expression pattern (data not shown).

Defects in branchial arch- and pouch-derived tissues

In the absence of the 2nd branchial arch in aaBb and aabb embryos, what are the effects on the formation of 2nd branchial arch-derived tissues? Most of the muscles that are needed for movement of eye lids, whiskers, ears, nose and lips are derived from paraxial mesoderm that migrates into the 2nd branchial arch (Trainor and Tam, 1995). Mice homozygous for the *Hoxa1* mutation (aaBB) show no apparent defects in the formation of facial muscles (Lufkin et al., 1991; Chisaka et al., 1992). *Hoxb1* mutant homozygotes (AAbb) show facial muscle paralysis and, in adults, these muscles degenerate; however, this syndrome results from defects in muscle innervation, rather than from a failure to form muscles during embryogenesis (Goddard et al., 1996). At birth, AAbb mice show normal facial musculature (Goddard et al., 1996). In the absence of a 2nd branchial arch (i.e., in aaBb and aabb newborn mice), most of the 2nd branchial arch-derived muscles are not formed. Fig. 3B,D illustrates the absence of the levator labii maxillaris, orbicularis occuli and zygomatic muscles in aabb newborn mice. The posterior belly of the digastric (pbd) and stylohyoid (sh) muscles, normally derived from the 2nd branchial arch, are formed, but as a single muscle that behaves, with respect to its points of connection, as a pbd muscle (Fig. 2D).

These results suggest that the 2nd branchial arch-derived muscles can be subdivided into two groups. The first, which are strictly involved in facial movements, have an absolute

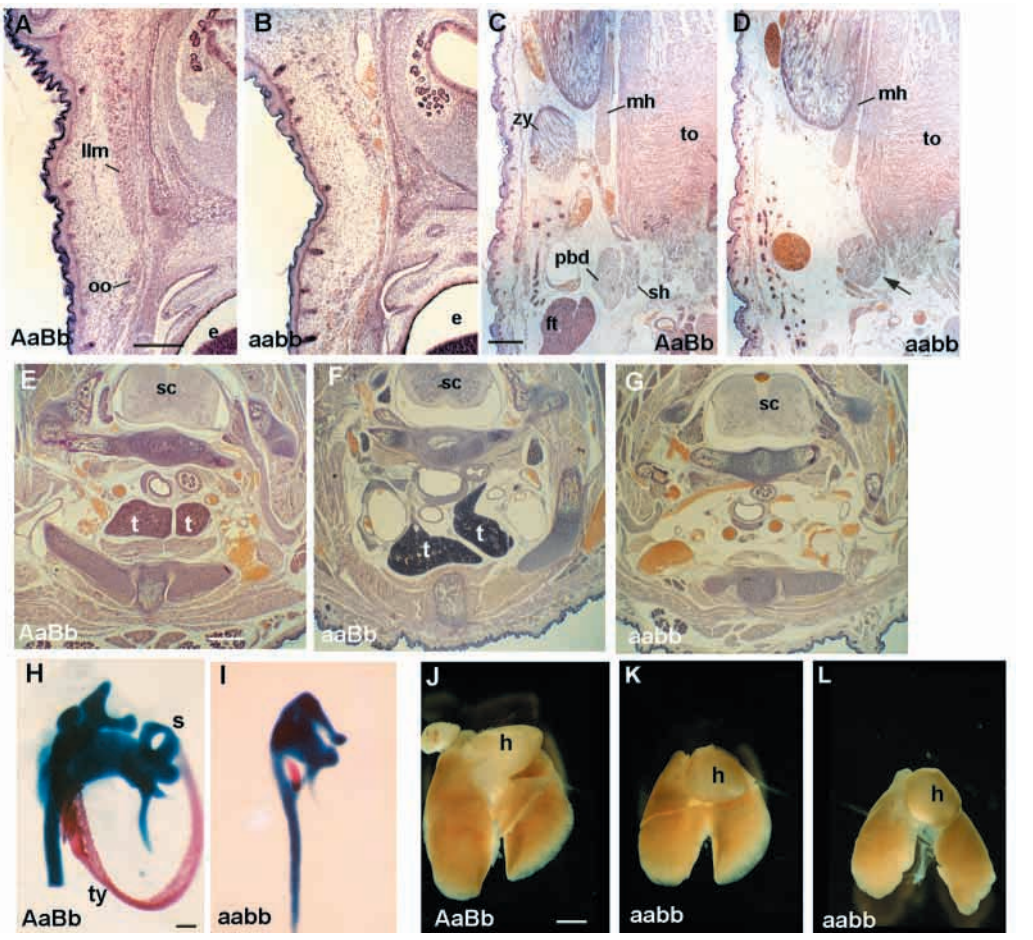

Fig. 3. Defects in branchial arch- and pouch-derived tissues. (A) Transverse section from a face of the newborn control mouse (AaBa) showing the position of the levator labii maxillaris (llm) and orbicularis occuli muscles (oo). (B) Comparable histological section from a *Hoxa1/Hoxb1* double mutant homozygous mouse shows the complete absence of these muscles. (C) This transverse section shows the positions of the zygomatic (zy), posterior belly of the digastric (pbd) and the stylohyoid (sh) muscles in control newborn mice. (D) In aabb mice, the zygomatic muscle is not present and the pbd and sh muscles are formed as a single muscle (arrow), which from its points of connection, behaves as a pbd muscle (see text). (E) The thymus (t) is derived from the third branchial pouch. (F) In aaBb embryos, the shape of the thymus is distorted relative to control embryos. (G) In aabb embryos, the thymus is not formed. (I) The middle ear components, derived from both the 1st and 2nd branchial arches, are highly hypoplastic in aabb relative to control newborn mice (H). The stapes (s), the only middle ear component derived from the 2nd branchial arch, is missing in aabb mice. Note also that only a vestige of the tympanic ring (ty) is formed in aabb mice. (J) The lung in newborn mice is composed of five lobes. (K,L) In aabb newborn mice, hypoplasia of lung formation is observed with variable expressivity ranging from five smaller lobes (K) to the formation of only two lobes (L). Scale bars A-D, 200 μm; E-G, 500 μm; H,I, 200 μm; J-L, 1000 μm.

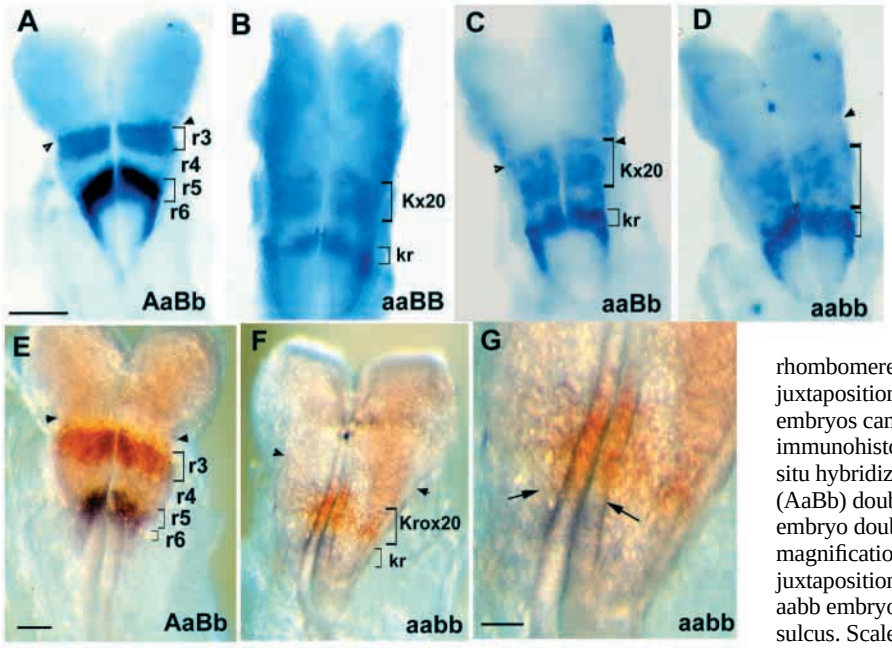

Fig. 4. Lack of rhombomeres 4 and 5 in aabb embryos. (A-D) E8.5 (4-9 somites) embryos hybridized with riboprobes to *Krox-20* (*Kx-20*) and *kreisler* (*kr*). (A) In control embryos, *Krox-20* and *kreisler* expression is observed in rhombomeres 3 and 5-6, respectively. (B) In aaBB embryos, the r3-Krox-20 expression is extended caudally and *kr* expression is restricted to a single rhombomere, rhombomere 6. (C) In aaBb embryos, the region between *Krox-20* and *kreisler* expression is reduced relative to aaBB embryos. (D) In aabb embryos, the boundaries of *Krox-20* and *kreisler* expression are juxtaposed. Thus, both rhombomeres 4 and 5 are missing in aabb embryos. (E-G) The juxtaposition of *Krox-20* and *kreisler* expression in aabb embryos can also be seen in embryos double labeled with immunohistochemistry (Krox-20: red brown label) and RNA in situ hybridization (kr: purple label). (E) E8.5 control embryo (AaBb) double labeled for *Krox-20* and *kreisler*. (F) E8.5 aabb embryo double labeled for *Krox-20* and *kreisler.* (G) Higher magnification of the embryo shown in F to emphasize the juxtaposition of the expression boundaries for these two genes in aabb embryos. Arrowheads indicate the position of the preotic sulcus. Scale bars, A-D, 200 μm; E, F, 100 μm; G, 54 μm.

requirement for the presence of the 2nd branchial arch for their formation. The second group, which are involved in throat movements, can form in the absence of the 2nd branchial arch, but are mispatterned. In aaBb and aabb mutants, the muscle precursors for the pbd and sh muscles may develop in the 3rd branchial arch, but may not be appropriately patterned because of the presence of 3rd branchial arch, rather than 2nd branchial arch neural crest. In the chick, Noden (1983a,b) has shown that neural crest patterns the craniofacial muscles.

Hoxa1 mutant homozygotes (aaBB) show defects in the formation of the middle and inner ear components derived from the 1st and 2nd branchial arches (Lufkin et al., 1991; Chisaka

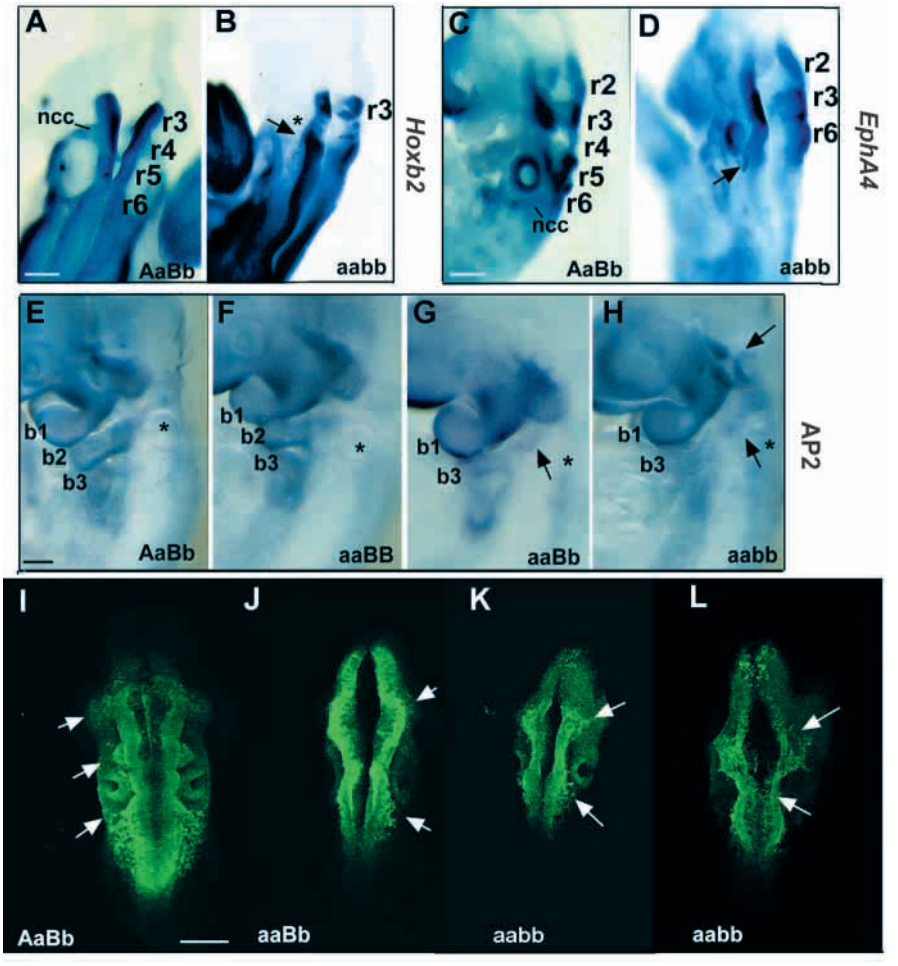

Fig. 5. Aberrant neural crest cell migration in aaBb and aabb embryos. (A,B) *Hoxb2* expression; (C,D) *EphA4* expression; (E-H) *AP-2* expression and (I-L) *CRABP1* expression. (A) In situ RNA hybridization pattern in an E9.5 control embryo with a *Hoxb2* riboprobe. *Hoxb2* is seen to be strongly expressed in the neural tube at the level of r3 to r5 and in neural crest emanating from r4 and r6. (B) In aabb embryos, *Hoxb2* expression is observed to be patchy in r3 and r6. The otic vesicle (asterisk) is at the level of r3/r6. No *Hoxb2*-labeled neural crest is observed to migrate from the preotic region of the neural tube, but a small strip of cells is seen coming from r6 dorsal to the otocyst and migrating caudally (arrow). (C) In situ hybridization of an E9.5 control embryo with *EphA4* riboprobe shows a strong signal in r3 and r5 and neural crest migrating from r6. (D) In double mutant homozygous embryos (aabb), strong r3-EphA4 expression is observed adjacent to strong r6 expression. A strip of neural crest expressing EphA4 is again observed at the level of r6 dorsal to the otocyst (arrow). (E) *AP-2* labels neural crest cells of E9.25-9.5 migrating into the 1st, 2nd and 3rd branchial arches, as well as the cranial sensory ganglia. (F) In aaBB embryos, a slight reduction of neural crest, labeled with *AP-2*, and migrating into the 2nd branchial arch is apparent. In aaBb (G) and aabb (H) embryos, *AP-2*-neural crest migrating into the 2nd arch is not observed. Particularly in aabb embryos, disorganization of the trigeminal ganglion is apparent. Neural crest cells migrating from the r2/3 region, but not reaching the 3rd branchial arch, are also observed (arrow) in aabb embryos. The asterisk marks the position of the otocyst. (I) A dorsal view of an E9.0 control embryo immunochemically reacted with a CRABP1 antibody showing the three major neural crest cell populations emanating from r2, r4 and r6 (arrows). (J) aaBb embryos at the same stage show only two populations of migratory neural crest, one at the r2/r3 level and the second caudal to the otocyst (i.e., from r6). (K,L) aabb embryos also show only two populations of migratory neural crest labeled with CRABP1. Scale bars (A-M), 200 μm; (I-L), 100 μm.

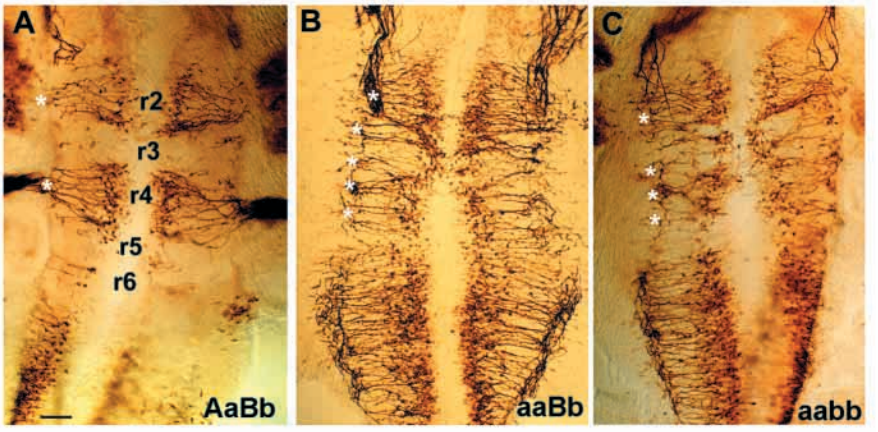

Fig. 6. Labeling of the branchiomotor neurons with an antibody to neurofilament protein. Differentiation of the branchiomotor neurons in the mouse hindbrain can be visualized as early as E9.5 using immunocytochemistry with an antibody directed to neurofilament protein. (A) In control embryos, viewed from the pial side, differentiation of these neurons can first be seen in r2 and r4, where the axons form fascicles and exit from a single point in each rhombomere. (B,C) In aaBb and aabb embryos, the early demarcation of differentiation of branchiomotor neurons among even and odd rhombomeres is not evident, the axons do not fasciculate and they exit at multiple points along the neural tube (asterisks). Scale bar, 100 μm.

et al., 1992). These defects are most readily interpreted in terms of deficiencies, rather than homeotic transformations. The expressivity of these deficiencies in aaBB newborn mice varies over a very wide range. In aaBb and aabb mice, the variation in expressivity of the middle and inner ear defects disappears, and all of the mutants exhibit the more extreme degree of hypoplasia seen in some aaBB mice. The stapes derived from the 2nd branchial arch is absent in aabb mice (Fig. 3I). However, it is also apparent from this figure that the malleus and the incus (derived from both 1st and 2nd branchial arches) are greatly reduced in size in aabb mice. Only a vestige of the tympanic ring, derived from the 1st branchial arch, is observed in aabb mice.

Not surprisingly, aaBb and aabb mice show defects in the formation of the external auditory meatus (see also Gavalas et al., 1998). Defects in the auditory meatus are apparent in *Hoxa1* mutant homozygotes and are extended in aaBb and aabb mice (data not shown). Of greater surprise is that the shape of the thymus is consistently distorted in aaBb mice and the thymus is missing in aabb mice (Fig. 3F,G). Also, parathyroids are not detected in either aaBb or aabb mice (data not shown). Both the thymus and parathyroid are derived from the 3rd branchial pouch endoderm, which is shifted in aaBb mice and distorted in aabb mice. These results indicate that, although the 3rd pouch endoderm is present in these mutant mice, it is not properly patterned.

Finally, we also observe a mutant phenotype in the lungs of aabb mice. The lung in newborn mice is composed of five lobes. In aabb mice, a hypoplasia of the lung is observed ranging from five smaller lobes, to only two lobes (Fig. 3K,L). Both *Hoxa1* and *Hoxb1* are expressed concurrently in the lung bud, beginning as early as E9.5 (Kappen, 1996; Mollard and Dziader, 1997). The histology of lung tissue in aabb mice appears grossly normal prior to birth, but the amount is reduced. It is of interest that *Hox* genes appear to be involved in controlling the growth of a number of tissues that expand by epithelial branching such as lungs, mammary tissue (Feng and Capecchi, 1999) and prostate (Podlasek et al., 1997).

Krox-20-kreisler expression

The *Hoxa1* component of the neural crest and branchial arch- and pouch-associated defects that we have just described in aaBb and aabb mice, must have their genesis in the disorganization of early hindbrain development. This follows because normal *Hoxa1* expression is restricted in the head region to the neural tube and ceases to be expressed there prior to emigration of the neural crest from the neural tube. For this reason, we have examined the organization of the hindbrain in these mutants using a series of molecular markers that distinguish rhombomeres (J. R. Barrow, H. S. Stadler, J. M. Goddard and M. C., unpublished results). Most informative among these markers are *Krox-20* and *kreisler.* At E8.5 (6-8 somites), *Krox-20* expression is seen in r3 and *kreisler* expression is present in r5 and 6 (Wilkinson et al., 1989; Cordes and Barth, 1994; Fig. 4A). Note that the r2-r3 boundary is marked by the position of the preotic sulcus, the r4 region is apparent by the bulge in that region of the hindbrain, and the r4-r5 boundary is at the level of the otic sulcus. *Krox-20* expression is patchy and extends much more caudally than normal in aaBB, aaBb and aabb embryos (Fig. 4B-D). In aaBB, aaBb and aabb embryos, *kreisler* expression is restricted to a single rhombomere, which from previous work is known to be rhombomere 6 (Carpenter et al., 1993; Mark et al., 1993). The region between *Krox-20* and *kreisler* expression has r4 identity as defined by *Hoxb1* expression. This region becomes increasingly smaller as we progress from aaBB to aaBb and to aabb embryos (Fig. 4B-D). In aabb embryos, the caudal boundary of *Krox-20* expression and the anterior boundary of *kreisler* expression are juxtaposed to each other. The juxtaposition of these two boundaries is also apparent in aabb embryos double labeled with an immunostain for *Krox-20* and an in situ probe for *kreisler* RNA (see Fig. 4F,G). The implication of these results is that both rhombomeres 4 and 5 are missing in aabb embryos. This deficiency is more extreme than that reported by Gavalas et al. (1998) for their *Hoxa1/Hoxb1* double mutant homozygotes.

The absence of an r4 domain would preclude formation of r4-derived neural crest. The absence of r4-derived neural crest could explain the selective loss of the 2nd branchial arch in aaBb and aabb embryos. We have used a series of molecular markers to determine directly whether r4-derived neural crest is detectable in aaBb and aabb embryos.

Hoxb2 and *EphA4* expression

At E9.5, *Hoxb2* is strongly expressed in rhombomeres 3, 4 and 5 and in the neural crest cells migrating from r4 and r6 into the 2nd and 3rd branchial arches, respectively (Hunt et al., 1991, Hunt and Krumlauf, 1991; Fig. 5A). In aaBb and aabb embryos, *Hoxb2* expression in r3 is patchy and discontinuous (Fig. 5B). The broad stripe of *Hoxb2*-labeled neural crest normally emanating from r4 and migrating ventrally to the 2nd branchial arch is not seen. Instead, at this position a small population of *Hoxb2*-labeled neural crest is migrating caudally. This population of neural crest is presumably r6-derived and attempting to migrate into the 3rd branchial arch. This migration is hindered by the presence of the otocyst. Even in aaBb embryos (E9.0-9.5), which retain one functional copy of the *Hoxb1* gene, no *Hoxb2*-labeled neural crest from the preotic region was observed to migrate into the branchial arch region (data not shown).

Similar results are observed using the gene encoding the tyrosine kinase receptor, *EphA4*, as a probe. *EphA4* is expressed weakly in r2 and r4 and strongly in r3 and r5 (Becker et al., 1994). It is also expressed in neural crest emanating from r6 and migrating to the 3rd branchial arch (Fig. 5C). In aaBb and aabb embryos, the r2 and r3 *EphA4* expression domains are visible but the r5 expression domain is not (Fig. 5D). The EphA4 neural crest cells emanating from r6, now at the level of the otic vesicle, are seen in the aabb embryos. To further examine the pattern of neural crest migration in aaBb and aabb mice, we studied the expression patterns of *AP-2* and *CRABP1*.

AP-2 and CRABP1 expression

Migratory and premigratory neural crest express the transcription factor AP-2 (Mitchell et al., 1991) and, in fact, mice with targeted disruptions in AP-2 show defects in neural crest-derived tissues (Schorle et al., 1996; Zhang et al., 1996). At E9.0-9.5, three populations of neural crest, labeled with AP-2, can be viewed in the branchial arch region migrating into the three branchial arches (Fig. 5E). The migration pattern and the amount of AP-2-labeled neural crest migrating into the branchial arches appears fairly normal in aaBB embryos (Fig.

5F). However, only two populations of neural crest migrating into the 1st and 3rd arch are visible in aaBb and aabb embryos (Fig. 5G,H).

The retinoic acid-binding protein (CRABP1) gene is also expressed by neural crest cells on the dorsal aspects of the neural tube and following their emanation from the neural tube (Maden et al., 1992; Ruberte et al., 1992). At E9.0, in control embryos labeled with an antibody directed against CRABP1, reveals three major streams of neural crest cells migrating to the three branchial arches (Fig. 5I). In aaBb and aabb embryos, only two streams of neural crest are seen migrating to the 1st and 3rd branchial arches (Fig. 5J-L). Taken together, these results suggest that, in both aaBb and aabb embryos, there is a major deficiency of neural crest emanating from the r4 region. The simplest hypothesis to account for this deficiency is that there is little or no r4 region that can function as a source for this neural crest cell population in aaBb and aabb mice, respectively.

Branchiomotoneurons within the hindbrain of aaBb and aabb embryos

The organization of the hindbrain in aaBb and aabb embryos has been further examined by visualizing the distribution of branchiomotoneurons labeled with a neurofilament antibody. These neurons differentiate within the mouse hindbrain as early as E9.5 (Lumsden and Keynes, 1989; McKay et al., 1994). The first branchiomotoneurons to differentiate are seen in rhombomeres 2 and 4, where they send fasciculated axons towards their respective exit points (Fig. 6A). The odd-numbered rhombomeres, r3 and r5, are delayed in the differentiation of their branchiomotor and reticular neurons; thus at this stage almost no neurons and axons expressing the neurofilament protein are observed in r3 and r5. In aaBb and aabb mutant embryos, no region of low neuron content is observed (Fig. 6B,C). Rhombomere 2 neurons are still recognizable in the mutant embryos because of the convergence of axons towards an exit point. However, branchiomotoneurons are present all along the hindbrain sending axons laterally and without extensive fasciculation to multiple exit points. These mutants have lost the characteristic hindbrain organization into distinct even- and odd-numbered rhombomeres. Similar, but less extensive heterochronicity of neural differentiation in the hindbrain of *Hoxa1* mutant embryos has recently been reported by Helmbacher et al. (1998).

We have also examined the organization of the hindbrain at E11-E11.5 by retrograde labeling of motoneurons with carbocyanine dyes (Carpenter et al., 1993; Goddard et al., 1996; data not shown). Our results are very similar to, and do not significantly extend, those already reported by Gavalas et al. (1998).

Roles of *Hoxa1* and *Hoxb1* in specification of rhombomere identity

From experiments using molecular markers to define rhombomere identity, it is apparent that, in early *Hoxa1* mutant embryos (E8.5-9.0), the region occupied by r3 (i.e., expressing *Krox-20*) is larger than normal. In addition, r4, the region expressing *Hoxb1,* is smaller than normal, and the r5 region, based on multiple markers, is entirely (Carpenter et al., 1993) or almost entirely (Mark et al., 1993) missing. In *Hoxa1/Hoxb1* double mutants, this aspect of the mutant phenotype is extended such that r4 is entirely (herein) or almost entirely (Gavalas et al., 1998) missing. The absence of r5 in *Hoxa1* mutants and r4 and r5 in *Hoxa1/Hoxb1* double mutants could result either from a failure of cell proliferation or cell specification, or from a failure to maintain rhombomeres after formation due, for example, to activation of apoptosis. J. R. Barrow, H. S. Stadler, J. M. Goddard and M. C. (unpublished data) suggest that r5 is missing in aaBB mutants because of misspecification that extends from r2 through r5. Specifically, *Hoxa1* activity is required to establish the anterior boundary of *Hoxb1* expression at the r3/r4 boundary. In the absence of *Hoxa1* activity, the *Hoxb1* anterior boundary is at a more caudal position, leading to a cascade of misspecification of rhombomeres that extends from r2 through r5 at the expense of specifying an r5 identity. This model arose from a careful examination of expression of *Krox-20, Hoxb1* and other molecular markers as a function of developmental time in normal and *Hoxa1* mutant embryos. Based on a set of embryonic morphological and molecular markers, it was observed that the length of the hindbrain in the early embryos (E8.0-E9.0) did not differ measurably between control and mutant embryos. Instead, what differed was the positions of the boundaries of expression of transcription factors involved in the specification of rhombomere identities relative to these morphological and molecular markers. Only later in embryogenesis (i.e., E8.5, onward) are size adjustments initiated in the misspecified hindbrain by induction of apoptosis leading to reductions in the length of the hindbrain of mutant embryos.

The pattern of *Hoxb1* expression cannot readily be followed in aabb embryos because of the absence of *Hoxb1* products (RNA and protein). Even in mutant alleles where a reporter gene (such as the green fluorescence protein, G. O. Gaufo, U. P. Flodby and M. C., unpublished results) has been introduced into the *Hoxb1* locus, its expression is rapidly turned off in the hindbrain due to a failure of *Hoxb1* autoregulation (Pöpperl et al., 1995). However, *Hoxb1* expression can be examined in aaBb embryos, which still retain one functional copy of *Hoxb1*. Fig. 7 shows results for experiments in which sequential double immunohistochemistry with polyclonal antibodies was used to display expression of *Krox-20* (green label) and *Hoxb1* (red label) proteins. In E8.5 aaBb embryos, *Hoxb1* expression is seen to be even more disorganized and extended more posteriorly than in aaBB embryos (Fig. 7B,C). By E10.0, when *Krox-20* ceases to be expressed in the hindbrain, aaBb mutant embryos show only a remnant of *Hoxb1*-expressing cells in the hindbrain, even though these embryos still retain one functional copy of *Hoxb1* (Fig. 7E).

Increase in programmed cell death

It is known that, at E9.5-E10.0, the length of the hindbrain is measurably shorter in *Hoxa1* mutant embryos than in normal controls (Carpenter et al., 1993; Mark et al., 1993). This shortening of the hindbrain is even more pronounced in aabb embryos. However, earlier in embryogenesis, E8.0-E8.5, the lengths of the hindbrains in aaBB and aabb embryos is not measurably different from those in controls (i.e., AABB or AaBb embryos). This implies that there is an adjustment in the length of the hindbrain in aaBB, aaBb and aabb embryos that commences ~E8.5. Interestingly, the initial adjustment of

length of the hindbrain that is observed in aaBB embryos by induction of apoptosis is seen in the r2/r3 region that displays extended *Krox-20* expression (J. R. Barrow, H. S. Stadler, J. M. Goddard and M. C., unpublished results). In aabb embryos, we observe an even more extended induction of apoptosis than is observed in aaBB embryos.

Whole-mount TUNEL assays were used to visualize apoptosis in the hindbrain (red labeling Fig. 8). In control embryos, apoptosis is observed along the dorsal ridge of the hindbrain of E8.5-E9.5 embryos and is associated with neural tube closure. Apoptosis is also observed in the population of neural crest cells migrating from the neural tube. To provide spatial reference, the embryos (A-D) were also stained with serum directed against Krox20 protein (green label). In aaBB

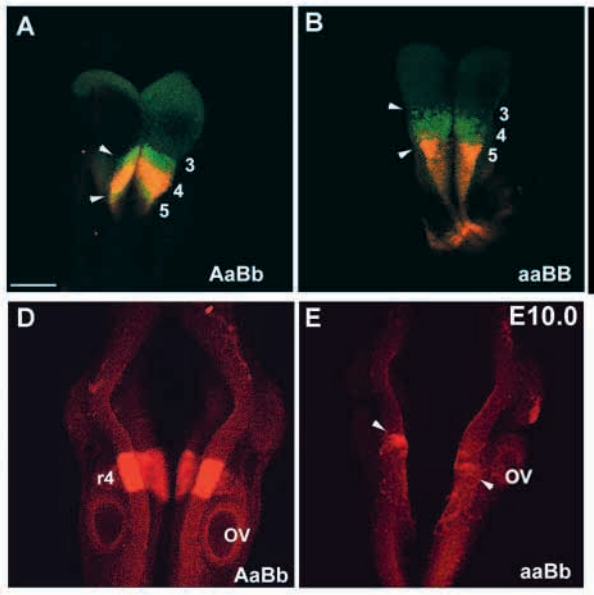

Fig. 7. Patterns of *Krox-20* and *Hoxb1* expression in early (E8.5) and later (E10.0) aaBb embryos. Sequential double immunochemistry with polyclonal antibodies directed against *Krox-20* (green label) and *Hoxb1* (red label) proteins was used to follow the expression of these genes in the neural tube of early embryos. (A) In control E8.5 embryos, *Krox-20* is strongly expressed in rhombomere 3 and is beginning to be expressed in rhombomere 5. The region occupied by rhombomere 4 is designated by *Hoxb1* expression. Morphologically this rhombomere is characterized by a bulge in the hindbrain. (B) Relative to morphological markers such as the preotic and otic sulci and the position of the first somite, the anterior boundary of *Hoxb1* expression in aaBB embryos is at a more posterior level than in control embryos. Also the r3-Krox-20 domain is larger and extends more posteriorly than in control embryos. (C) The anterior boundary of *Hoxb1* expression and the caudal boundary of Krox-20 expression are extended even more posteriorly in aaBb embryos than in aaBB embryos. (D) By E10.0, Krox-20 ceases to be expressed in the neural tube of control embryos, but strong expression of *Hoxb1* in the region occupied by rhombomere 4 is observed. Neural crest cells emanating from r4 are also expressing *Hoxb1*. (E) At E10.0, aaBb embryos show only a vestige of cells in the neural tube expressing *Hoxb1*, even though these embryos still retain one functional copy of *Hoxb1*. Note the position of the otocyst relative to the position of the preotic sulcus. Scale bar, 100 μm.

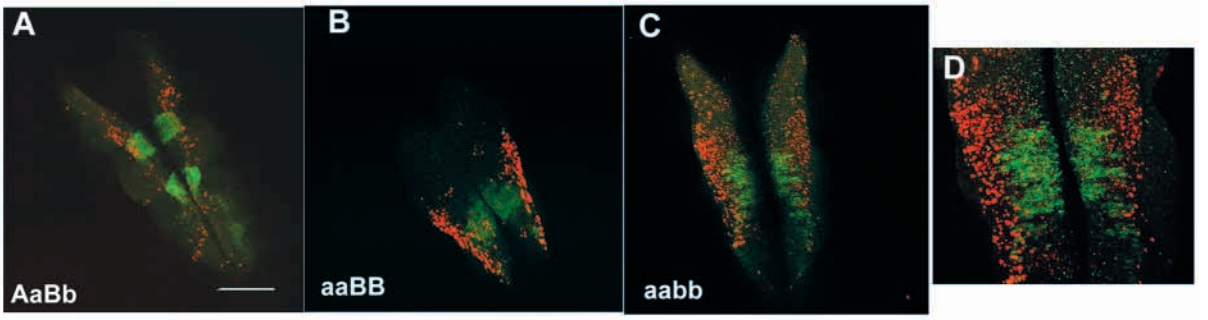

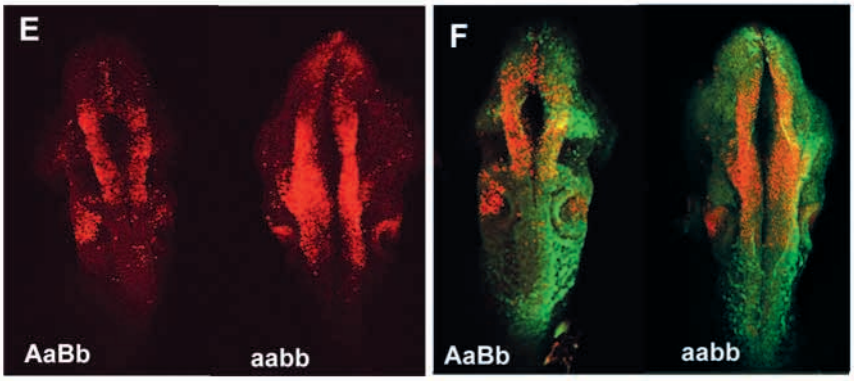

Fig. 8. Adjustment of brain length in aaBB and aabb mutant embryos by induction of apoptosis. The level of apoptosis in control and mutant hindbrains was assessed by whole-mount TUNEL assays. For A-D, immunochemical staining of *Krox-20* (green) was included to serve as a molecular landmark. (A-D) The TUNEL assays were performed on E9.0 (10-11 somites) embryos. The level of apoptosis in aaBB embryos (B) is increased relative to control embryos (A; see also accompanying paper by Barrow et al., 1999). (C) The level of apoptosis in aabb embryos is seen to be even further increased, and the increase extends more posteriorly in aabb embryos relative to aaBB embryos. Note that, at a higher magnification, apoptotic cells can be seen throughout the neural epithelium of aabb mice (D). (E,F) The TUNEL assays were performed on E9.5 (20-25 somite) embryos. (F) The embryos were immunochemically reacted with antisera directed against CRABP1, again to serve as a molecular reference point. A delay in neural tube closure is evident in aabb embryos relative to controls. It is seen that, at this stage, increased apoptosis in aabb embryos is present through the hindbrain neural tube. For each embryonic period, four embryos of each genotype were examined by TUNEL assay to determine the extent of apoptosis. Scale bar, 100 μm.

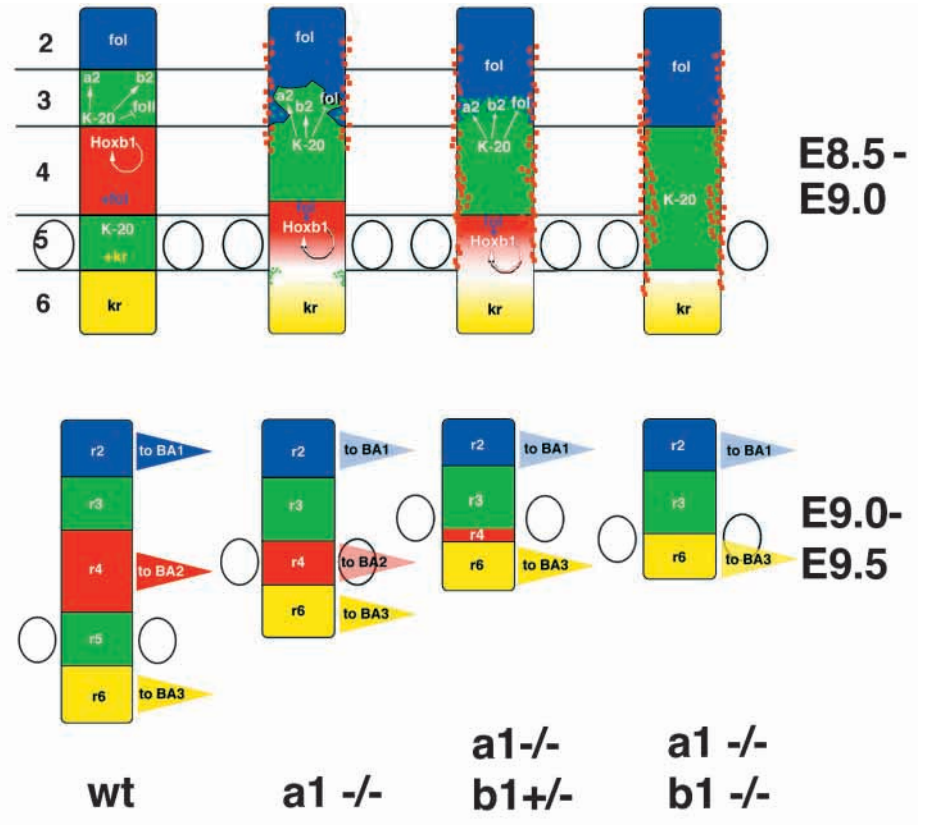

Fig. 9. A model for how mutations in *Hoxa1* and *Hoxb1* result in disruption of hindbrain organization. The details of this model are described in the accompanying paper by Barrow et al. (1999). However, the principal points are that the reason that *Hoxa1* mutants (aaBB) and *Hoxa1/Hoxb1* double mutants (aabb) fail to form rhombomere 5 and rhombomere 4 and 5, respectively, is not because of a failure in cell proliferation and/or maintenance of these rhombomeres, but rather from a failure in rhombomere specification. Specifically, in aaBB mutants, the lack of formation of rhombomere 5 is a consequence of extending caudally the region expressing r3 and r4-specific markers into the region normally occupied by r5. As a consequence, r5 fails to be specified at the expense of forming cells with an r4 identity. In the double mutants (aabb), this process is pushed even farther since, in the absence of *Hoxb1*, no rhombomere 4 region is specified and therefore the r3-Krox-20 region extends even more caudally to rhombomere 6. In the absence of *Hoxb1* and *Hoxa1*, both rhombomere 4 and 5 fail to be specified. Subsequent to this failure in specification, and overspecification of the region expressing rhombomere 2 and 3 markers, apoptosis is induced in an attempt to regulate the imbalance of specification in these mutant hindbrains.

embryos, *Krox20* expression is limited to a single band (r3) that is broader and extends to a more posterior level than in control embryos (Carpenter et al., 1993; J. R. Barrow, H. S. Stadler, J. M. Goddard and M. C., unpublished results). In aaBB E9.0 embryos, an increased level of apoptosis is observed in the rostral hindbrain (Fig. 8B). The number of apoptotic cells is extended posteriorly in the neuroepithelium of E9.0, aabb embryos (Fig. 8C,D). The increase in the level of apoptosis in aabb embryos is also evident at later stages of embryogenesis (Fig. 8E,F). At E9.5, apoptosis is normally observed to extend into the alar plate of the neural tube, in migrating neural crest cells and in the region of the otocyst where the endolymphatic duct will form. At this stage, the level of apoptosis is again observed to be greater and more extended in the neural tube of aabb embryos. The embryos in F were immunoreacted with an antibody directed against CRABP1 to mark the position of migrating neural crest cells (green labeling).

To determine if the patterns of cell proliferation differed measurably between controls and aabb embryos, incorporation of BrdU was assessed in E9.5 and E10.0 embryos (see Materials and Methods). No differences in the level or pattern of BrdU incorporation were discernible between control and mutant (aabb) embryos (data not shown). In particular, there did not appear to be any gaps or reductions of BrdU labeling in the r4/r5 region of aabb embryos. Thus, the absence of molecular markers that normally define the identities of r4 and r5 in aabb embryos, could not be ascribed to a defect in cell proliferation in this region. For these assays, two embryos of each genotype and at each time point were sectioned and processed for BrdU incorporation.

DISCUSSION

The consequences to the development of the hindbrain that result from individual mutations in *Hoxa1* or *Hoxb1* are very different. *Hoxa1* mutant homozygotes show marked defects in the metameric organization of the developing hindbrain. In these mutant embryos, rhombomere 3 is excessively large, rhombomere 4 is reduced in size and rhombomere 5 is either entirely (Carpenter et al., 1993) or almost entirely (Mark et al., 1993) missing. In contrast, disruption of *Hoxb1* does not alter the metameric pattern of the developing hindbrain, but instead affects the fate of neurons within rhombomere 4 (Goddard et al., 1996; Studer et al., 1996). These distinct differences in mutant phenotype suggested separate roles for these two paralogous *Hox* genes in hindbrain development. However, analysis of mice mutant for both *Hoxa1* and *Hoxb1* demonstrates extensive overlap in function between these two genes. The disruption in rhombomere organization observed in *Hoxa1* mutant embryos is exacerbated by the removal of one or both functional copies of the *Hoxb1* gene. In addition, although *Hoxa1* mutant homozygotes show mild hypoplasia of the 2nd branchial arch, in aaBb or aabb mutant embryos, the 2nd branchial arch is completely missing. These are but two examples of affected tissues and structures observed in *Hoxa1/Hoxb1* double mutants that demonstrate extensive overlap of functions between these two paralogous *Hox* genes. Such overlap in function suggests commonality in mechanism of action for these two genes.

Fig. 9 illustrates a model for hindbrain development in which the roles of *Hoxa1* and *Hoxb1* are very similar. It is proposed that the function of both genes in the early hindbrain

is to specify rhombomere identity and that the differences in the mutant phenotypes resulting from individual disruption of these genes arise because *Hoxa1,* in addition to its normal role in specifying rhombomere identities, is also required to extend the anterior boundary of *Hoxb1* to the presumptive r3/r4 boundary. In the absence of *Hoxa1* function, the anterior boundary of *Hoxb1* is within the normal r4 territory rather than at the r3/r4 presumptive boundary. This in turn leads to misspecifications of the normal rhombomere 3 and rhombomere 5 territories. A main feature of the model is that the unique roles attributable to *Hoxa1* and *Hoxb1* do not arise from separate protein functions, but rather from differences in their kinetics of gene expression. *Hoxa1* is expressed first and reaches the presumptive r3/r4 boundary first. Having reached this anterior boundary, it participates in activating *Hoxb1* expression at this anterior level. In the absence of *Hoxa1* activity, *Hoxb1* expression never reaches this anterior boundary and specification of rhombomere 4 is incomplete and occurs at a more caudal level than normal.

Subsequent to misspecification of the hindbrain in aaBB, aaBb and aabb embryos, apoptosis appears to be used to initiate size adjustment within the misspecified hindbrain. Similar adjustments in size by apoptosis have been noted in *kreisler* mutants (McKay et al., 1994). In the absence of *kreisler* function, *Hoxb1* is expressed in rhombomere 5, extending the rhombomere 4 territory to encompass both rhombomeres 4 and 5. Subsequent to this misspecification, induction of apoptosis is used to regulate the size of this aberrant region of the hindbrain. It remains to be determined which parameters are used to assess the need for size adjustments by apoptosis. Clearly apoptosis is initiated much earlier than the times when the neurons born in the affected territories innervate their normal targets.

As already pointed out, the kinetics of expression of *Hoxa1* and *Hoxb1* during embryogenesis are very different. *Hoxa1* reaches its anterior limit of expression in the hindbrain by E8.0, then commences to regress caudally and, by E8.5, there is no longer any *Hoxa1* expression in the head region of the embryo. *Hoxb1* expression, on the contrary, reaches the same anterior limit of expression just after *Hoxa1,* then regression of expression commences caudally from the hindbrain; however, a stripe of *Hoxb1* expression is retained in rhombomere 4. This expression pattern is dependent on the establishment of a *Hoxb1*-dependent autoregulatory loop (Pöpperl et al., 1995). These expression patterns suggest that *Hoxa1* only has an early function during the development of the hindbrain, whereas the continued presence of *Hoxb1* is needed for the proper specification of r4 neurons. Indeed, loss-of-function mutations in *Hoxb1* affect the identity and function of multiple groups of r4 neurons, including somatic and visceral motoneurons as well as sensory neurons. Thus the role in hindbrain development is more complex for *Hoxb1* than for *Hoxa1,* with *Hoxb1* having both an early and a more prolonged role during development. This difference in complexity may result from *Hoxb1*'s ability to control maintenance of its own transcription.

Hoxb1 mutant homozygotes show no defects in neural crest-derived tissues (Goddard et al., 1996; Studer et al., 1996), and *Hoxa1* mutants exhibit, with variable expressivity and penetrance, hypoplasia in neural crest-derived tissues associated with the 1st and 2nd branchial arches (Lufkin et al., 1991; Chisaka et al., 1992). *Hoxa1/Hoxb1* double mutant homozygotes, on the contrary, show complete absence of the 2nd branchial arch and complete deficiencies in many 1st and 2nd branchial arch-, as well as 2nd and 3rd branchial pouch-, derived tissues (Gavalas et al., 1998 and herein). These defects are most readily explained by a defect in the formation of r4 neural crest. In addition to the complete absence (herein) or almost complete absence (Studer et al., 1998) of an r4 territory capable of producing r4-derived neural crest, a variety of molecular markers that normally label this neural crest cell population are not observed in aaBb and aabb embryos.

Interestingly, in the chick, the consequence of physical ablation of this neural crest population could be compensated for by surrounding neural crest (Saldivar et al., 1997; Couly et al., 1996, 1998). With genetic ablation in the mouse, neither we nor Gavalas et al. (1998), observed compensation for the missing r4 neural crest by the surrounding neural crest. This difference in response may reflect a difference in the timing of the physical and genetic ablations. In the case of the chick, the physical ablations of the source of neural crest are done very early in development, providing a window of opportunity for compensation by the surrounding neural crest. The consequences of genetic ablation may not be felt until the need for the r4-derived neural crest arises, leaving insufficient time for compensation by the surrounding neural crest.

In the absence of formation of the 2nd branchial arch, it is not surprising that 2nd branchial arch-derived tissues are not found in aabb embryos. But the set of defects observed in aaBb and aabb embryos is more complex than simple deletions of 2nd branchial arch-derived tissues. Rather than deletion of all 2nd arch-derived muscles, the defects can be broken down into two groups. The derivatives strictly involved in facial musculature are absent. However, the more posterior 2nd arch-derived muscles are present, but improperly patterned. Also, extensive hypoplasia of 1st arch-derived tissues are evident in *Hoxa1/Hoxb1* double mutants. This includes the formation of only a vestige of the tympanic ring, the malleus and so on. These deficiencies in 1st arch-derived structure may reflect an indirect role of *Hoxa1* and *Hoxb1* in controlling the fate of cells in the anterior neural tube (Helmbacher et al., 1998). It may also reflect the fact that the normal morphological interactions between the newly forming tissues derived from these two arches are so interdependent that a failure in the formation of 2nd arch structures also affects formation of 1st arch structures. An additional possibility is that the ectopic apoptosis observed in the r2/r3 region of the neural tube of aaBB, aaBb and aabb embryos results in a reduction in the production of r2-neural crest. This reduction would manifest itself in hypoplasia of 1st branchial arch-derived tissues. Defects caudal to the 2nd branchial arch are also evident in aabb newborn mice. Most surprising is the absence of a thymus and parathyroid, normally derived from the 3rd branchial pouch. These defects are seen in *Hoxa3* mutant homozygotes (Chisaka and Capecchi, 1991) but were not suspected to be associated with mutations in *Hoxa1* and *Hoxb1*. The expression pattern of *Hoxa3* in the branchial region appears normal in aabb embryos (data not shown), but the morphology of the 3rd branchial pouch is perturbed in the *Hoxa1/Hoxb1* double mutant embryos.

In summary, the disorganization in the patterning of the r4/r5 presumptive territories in aabb embryos results in a failure to form the neural crest needed for the formation of the 2nd branchial arch. This in turn results in deficiencies in forming

both 2nd arch- and 2nd pouch-derived tissue as well as 1st arch- and 3rd pouch-derived tissues. We suggest that hindbrain defects result from a failure in rhombomere specification initiated by the absence of *Hoxa1* gene product, but compounded by the additional absence of *Hoxb1* gene product. The *Hoxa1/Hoxb1* double mutant provides a clear example of misspecification of hindbrain segmentation leading to a cascade of developmental defects that result in major malformations in craniofacial development.

We thank J. Goddard and S. Barnett for the preparation of the $Hoxb1^{BloxP}$ allele of *Hoxb1*, H. S. Stadler for advice on the TUNEL analysis, E. King and the Imaging Facility in the Department of Biology for assistance with scanning electron microscopy, and L. Oswald for help in the preparation of this manuscript. M. R. was an associate of the Howard Hughes Medical Institute. The 3H3 neurofilament hybridoma was obtained from the Developmental Studies Hybridoma Bank under contract No. 1-HD-6-2915 from the NICHD.

REFERENCES

Araki, K., Araki, M., Miyazaki, J.-I. and Vassalli, P. (1995). Site-specific recombination of a transgene in fertilized eggs by transient expression of Cre recombinase. *Proc. Natl. Acad. Sci. USA* **92**, 160-164.

Barrow, J. R. and Capecchi, M. R. (1999). Compensatory defects associated with mutations in *Hoxa1* restore normal palatogenesis to *Hoxa2* mutants. *Development* **126,** In press.

Becker, N., Seitanidou, T., Murphy, P., Mattéi, M.-G., Topilko, P., Nieto, M. A., Wilkinson, D. G., Charnay, P. and Gilardi-Hebenstreit, P. (1994). Several receptor tyrosine kinase genes of the *Eph* family are segmentally expressed in the developing hindbrain. *Mech. Dev.* **47**, 3-17.

Blum, M., Gaunt, S. J., Cho, K. W., Steinbeisser, H., Blumberg, B., Bittner, D. and Robertis, E. M. D. (1992). Gastrulation in the mouse: the role of the homeobox gene goosecoid. *Cell* **69**, 1097-1106.

Carpenter, E. M., Goddard, J. M., Chisaka, O., Manley, N. R. and Capecchi, M. R. (1993). Loss of *Hox-A1* (*Hox-1.6*) function results in the reorganization of the murine hindbrain. *Development* **118**, 1063-1075.

Chen, F. and Capecchi, M. R. (1999). The paralogous mouse *Hox* genes, *Hoxa9*, *Hoxb9* and *Hoxd9*, function together to control development of the mammary gland in response to pregnancy. *Proc. Natl. Acad. Sci. USA* **96**, 541-546.

Chisaka, O. and Capecchi, M. R. (1991). Regionally restricted developmental defects resulting from targeted disruption of the mouse homeobox gene *hox-1.5*. *Nature* **350**, 473-479.

Chisaka, O., Musci, T. S. and Capecchi, M. R. (1992). Developmental defects of the ear, cranial nerves and hindbrain resulting from targeted disruption of the mouse homeobox gene *Hox-1.6*. *Nature* **355**, 516-520.

Cordes, S. P. and Barsh, G. S. (1994). The mouse segmentation gene *kr* encodes a novel basic domain-leucine zipper transcription factor. *Cell* **79**, 1025-1034.

Couly, G., Grapin-Botton, A., Coltey, P. and Le Douarin, N. M. (1996). The regeneration of the cephalic neural crest, a problem revisited: the regenerating cells originate from the contralateral or from the anterior and posterior neural fold. *Development* **122**, 3393-3407.

Couly, G., Grapin-Botton, A., Coltey, P., Ruhin, B. and Le Douarin, N. M. (1998). Determination of the identity of the derivatives of the cephalic neural crest: incompatibility between *Hox* gene expression and lower jaw development. *Development* **125**, 3445-3459.

Dodd, J., Morton, S. B., Karagogeos, D., Yamamoto, M. and Jessell, T. M. (1988). Spatial regulation of axonal glycoprotein expression on subsets of embryonic spinal neurons. *Neuron* **1**, 105-116.

Eriksson, U., Hansson, E., Nordlinder, H., Busch, C., Sundelin, J. and Peterson, P. A. (1987). Quantitation and tissue localization of the cellular retinoic acid-binding protein. *J. Cell. Physiol.* **133**, 482-490.

Feng, C. and Capecchi, M. R. (1999). Paralogous mouse *Hox* genes, *Hoxa9*, *Hoxb9*, and *Hoxd9*, function together to control development of the mammary gland in response to pregnancy. *Proc. Natl. Acad. Sci. USA* **96**, 541-546.

Fraser, S., Keynes, R. and Lumsden, A. (1990). Segmentation in the chick embryo hindbrain is defined by cell lineage restrictions. *Nature* **344**, 431-435.

Frohman, M. A., Boyle, M and Martin, G. R. (1990). Isolation of the mouse *Hox-2.9* gene; analysis of embryonic expression suggests that positional information along the anterior-posterior axis is specified by mesoderm. *Development* **110**, 589-607.

Gaunt, S. J., Blum, M. and De Robertis, E. M. (1993). Expression of the mouse goosecoid gene during mid-embryogenesis may mark mesenchymal cell lineages in the developing head, limbs and body wall. *Development* **117**, 769-778.

Gavalas, A., Studer, M., Lumsen, A., Rijli, F. M., Krumlauf, R. and Chambon, P. (1998). *Hoxa1* and *Hoxb1* synergize in patterning the hindbrain, cranial nerves and second pharyngeal arch. *Development* **125**, 1123-1136.

Gendron-Maguire, M., Mallo, M., Zhang, M. and Gridley, T. (1993). *Hoxa-2* mutant mice exhibit homeotic transformation of skeletal elements derived from cranial neural crest. *Cell* **75**, 1317-1331.

Goddard, J. M., Rossel, M., Manley, N. R. and Capecchi, M. R. (1996). Mice with targeted disruption of *Hoxb-1* fail to form the motor nucleus of the VIIth nerve. *Development* **122**, 3217-3228.

Godwin, A. R., Stadler, H. S., Nakamura, K. and Capecchi, M. R. (1998). Detection of targeted *GFP-Hox* gene fusions during mouse embryogenesis. *Proc. Natl. Acad. Sci. USA* **95**, 13042-13047.

Helmbacher, F., Pujades, C., Desmarquet, C., Frain, M., Rijli, F. M., Chambon, P. and Charnay, P. (1998). *Hoxa1* and *Krox-20* synergize to control the development of rhombomere 3. *Development* **125**, 4739-4748.

Hunt, P., Gulisano, M., Cook, M., Sham, M.-H., Faiella, A., Wilkinson, D., Boncinelli, E. and Krumlauf, R. (1991). A distinct *Hox* code for the branchial region of the vertebrate head. *Nature* **353**, 861-864.

Hunt, P. and Krumlauf, R. (1991). Deciphering the hox code: clues to patterning branchial regions of the head. *Cell* **66**, 1075-1078.

Kappen, C. (1996). Hox genes in the lung. *Am. J. Respir. Cell Mol. Biol.* **15**, 156-162.

Köntges, G. and Lumsden, A. (1996). Rhombencephalic neural crest segmentation is preserved throughout craniofacial ontogeny. *Development* **122**, 3229-3242.

LaRosa, G. J. and Gudas, L. J. (1988). Early retinoic acid induced F9 teratocarcinoma stem cell gene ERA-1: alternate splicing creates transcripts for a homeobox-containing protein and one lacking the homeobox. *Mol. Cell. Biol.* **8**, 3906-3917.

Le Lievre, C. S. and Le Douarin, N. M. (1975). Mesenchymal derivatives of the neural crest: analysis of chimaeric quail and chick embryos. *J. Embryoll. exp. Morph.* **34**, 125-154.

Lufkin, T., Dierich, A., LeMeur, M., Mark, M. and Chambon, P. (1991). Disruption of the *Hox-1.6* homeobox gene results in defects in a region corresponding to its rostral domain of expression. *Cell* **66**, 1105-1119.

Lumsden, A. and Keynes, R. (1989). Segmental patterns of neuronal development in the chick hindbrain. *Nature* **337**, 424-428.

Lumsden, A., Sprawson, N. and Graham, A. (1991). Segmental origin and migration of neural crest cells in the hindbrain region of the chick embryo. *Development* **113**, 1281-1291.

Maden, M., Horton, C., Graham, A., Leonard, L., Pizzey, J., Siegenthaler, G., Lumsden, A. and Eriksson, U. (1992). Domains of cellular retinoic acid-binding protein I (CRABP I) expression in the hindbrain and neural crest of the mouse embryo. *Mech. Dev.* **37**, 13-23.

Maden, M., Graham, A., Gale, E., Rollinson, C. and Zile, M. (1997). Positional apoptosis during vertebrate CNS development in the absence of endogenous retinoids. *Development* **124**, 2799-2805.

Manley, N. R. and Capecchi, M. R. (1995). The role of *hoxa-3* in mouse thymus and thyroid development. *Development* **121**, 1989-2003.

Manley, N. R. and Capecchi, M. R. (1997). *Hox* group 3 paralogous genes act synergistically in the formation of somitic and neural crest-derived structures. *Dev. Biol.* **192**, 274-288.

Manley, N. R. and Capecchi, M. R. (1998). *Hox* group 3 paralogs regulate the development and migration of the thymus, thyroid and parathyroid glands. *Dev. Biol.* **195**, 1-15.

Mansour, S. L., Goddard, J. M. and Capecchi, M. R. (1993). Mice homozygous for a targeted disruption of the proto-oncogene *int-2* have developmental defects in the tail and inner ear. *Development* **117**, 13-28.

Mark, M., Lufkin, T., Vonesch, J.-L., Ruberte, E., Olivo, J.-C., Dollé, P., Gorry, P., Lumsden, A. and Chambon, P. (1993). Two rhombomeres are altered in *Hoxa-1* mutant mice. *Development* **119**, 319-338.

McKay, I. J., Muchamore, I., Krumlauf, R., Maden, M., Lumsden, A. and Lewis, J. (1994). The *kreisler* mouse: a hindbrain segmentation mutant that lacks two rhombomeres. *Development* **120**, 2199-2211.

Mitchell, P. J., Timmons, P. M., Hebert, J. M., Rigby, P. W. and Tijian, R. (1991). Transcription factor AP-2 is expressed in neural crest cell lineages during mouse embryogenesis. *Genes Dev.* **5**, 105-110.

Mollard, R. and Dziadek, M. (1997). Homeobox genes from clusters A and B demonstrate characteristics of temporal colinearity and differential restrictions in spatial expression domains in the branching mouse lung. *Int. J. Dev. Biol.* **41**, 655-666.

Moser, M., Ruschoff, J. and Buettner, R. (1997). Comparative analysis of AP-2 alpha and AP-2 beta gene expression during murine embryogenesis. *Dev. Dyn.* **208**, 115-124.

Murphy, P. and Hill, R. E. (1991). Expression of the mouse *labial*-like homeobox-containing genes, *Hox 2.9* and *Hox 1.6*, during segmentation of the hindbrain. *Development* **111**, 61-74.

Noden, D. M. (1983a). The embryonic origins of avian cephalic and cervical muscles and the associated Connective tissues. *Am. J. Anat.* **168**, 257-276.

Noden, D. M. (1983b). The role of the neural crest in patterning of avian cranial skeletal, connective and muscle tissues. *Dev. Biol.* **96**, 144-165.

Podlasek, C. A., Duboule, D. and Bushman, W. (1997). Male accessory sex organ morphogenesis is altered by loss of function of *Hoxd-13*. *Dev. Dyn.* **208**, 454-465.

Pöpperl, H., Bienz, M., Studer, M., Chan, S.-K., Aparicio, S., Brenner, S., Mann, R. S. and Krumlauf, R. (1995). Segmental expression of *Hoxb-1* is controlled by a highly conserved autoregulatory loop dependent upon *exd/pbx*. *Cell* **81**, 1031-1042.

Porteus, M. H., Brice, A. E., Bulfone, A., Usdin, T. B., Ciaranello, R. D. and Rubenstein, J. L. (1992). Isolation and characterization of a library of cDNA clones that are preferentially expressed in the embryonic telencephalon. *Brain Res. Mol. Brain Res.* **12**, 7-22.

Rijli, F. M., Mark, M., Lakkaraju, S., Dierich, A., Dollé, P. and Chambon, P. (1993). A homeotic transformation is generated in the rostral branchial region of the head by disruption of *Hoxa-2*, which acts as a selector gene. *Cell* **75**, 1333-1349.

Ruberte, E., Friederich, V., Morris-Kay, G. and Chambon, P. (1992). Differential distribution patterns of CRABP1 and CRABP2 transcripts during mouse embryogenesis. *Development* **115**, 973-987.

Saldivar, J. R., Sechrist, J. W., Krull, C. E., Ruffins, S. and Bronner-Fraser, M. (1997). Dorsal hindbrain ablation results in rerouting of neural crest migration and changes in gene expression, but normal hyoid development. *Development* **124**, 2729-2739.

Schneider-Maunoury, S., Topilko, P., Seitanidou, T., Levi, G., Cohen-Tannoudji, M., Pournin, S., Babinet, C. and Charnay, P. (1993). Disruption of *Krox-20* results in alteration of rhombomeres 3 and 5 in the developing hindbrain. *Cell* **75**, 1199-1214.

Schorle, H., Meier, P., Buchert, M., Daenisch, R. and Mitchell, P. J. (1996). Transcription factor AP-2 essential for cranial closure and craniofacial development. *Nature* **381**, 235-238.

Schwenk, F., Baron, U. and Rajewsky, K. (1995). A *cre*-transgenic mouse strain for the ubiquitous deletion of *loxP*-flanked gene segments including deletion in germ cells. *Nucleic Acids Res.* **23**, 5080-5081.

Studer, M., Lumsden, A., Ariza-McNaughton, L., Bradley, A. and Krumlauf, R. (1996). Altered segmental identity and abnormal migration of motor neurons in mice lacking *Hoxb-1*. *Nature* **384**, 630-634.

Studer, M., Gavalas, A., Marxhall, H., Ariza-McNaughton, L., Rijli, F. M., Chambon, P. and Krumlauf, R. (1998). Genetic interactions between *Hoxa1* and *Hoxb1* reveal new roles in regulation of early hindbrain patterning. *Development* **125**, 1025-1036.

Trainor, P. A. and Tam, P. P. (1995). Cranial paraxial mesoderm and neural crest cells of the mouse embryo: co-distribution in the craniofacial mesenchyme but distinct segregation in branchial arches. *Development* **121**, 2569-2582.

Wallin, J., Eibel, H., Neubuser, A., Wilting, J., Koseki, H. and Balling, R. (1996). Pax1 is expressed during development of the thymus epithelium and is required for normal T-cell maturation. *Development* **122**, 23-30.

Wilkinson, D. G., Bhatt, S., Chavrier, P., Bravo, R. and Charnay, P. (1989). Segment-specific expression of a zinc-finger gene in the developing nervous system of the mouse. *Nature* **337**, 461-464.

Zhang, J., Hagopian-Donaldson, S., Serbedzija, G., Elsemore, J., Plehn-Dujowich, D., McMahon, A. P., Flavell, R. A. and Williams, T. (1996). Neural tube, skeletal and body wall defects in mice lacking transcription factor AP-2. *Nature* **381**, 238-241.